Physically and Mineralogically Based Spectroscopic Dielectric Model for Moist Soils

Valery L. Mironov, *Member, IEEE*, Lyudmila G. Kosolapova, and Sergej V. Fomin

***Abstract*—In this paper, the error of dielectric predictions for moist soils was estimated, regarding the semiempirical mixing dielectric model (SMDM) developed by Dobson *et al.*, which is a universally recognized one, and the generalized refractive mixing dielectric model (GRMDM) recently elaborated by Mironov *et al.* The analysis is based on the measured dielectric data presented in by Curtis *et al.* and the papers of Dobson *et al.* These data cover a broad variety of grain-size distributions observed in 15 soils and the frequency range from 45 MHz to 26.5 GHz, with the temperature being from 20 °C to 22 °C. The SMDM was found to deliver predictions with substantially larger error for the soils, whose dielectric data were not used for its development, while the GRMDM ensured dielectric predictions for all the soils analyzed with as small error as the SMDM did in the case of the soils that it was based on. To secure the same convenience in application of the GRMDM, which the SMDM possesses, the spectroscopic parameters of that model were correlated with the clay percentages of the respective soils. As a result, a new mineralogy-based dielectric model was developed. For the moist soils other than those whose dielectric data were used for its development, this model was shown to demonstrate noticeably smaller error of dielectric predictions, with clay percentage being the only input parameter, as compared with the error observed in the case of the SMDM.**

***Index Terms*—Complex dielectric constant (CDC), dielectric model, microwaves, moist soil.**

I. Introduction

Dielectric models of soils are an essential part of the algorithms used for data processing in radar and radio thermal remote sensing. At present, the semiempirical mixing dielectric model (SMDM) proposed in [1]–[3] has become a universally recognized mean for predicting the dielectric spectra of moist soils in the microwave band. To account for frequency dispersion of moist-soil complex dielectric constant (CDC), the SMDM uses the Debye relaxation spectrum of liquid water, which is located out of soil. With this approach, implying that the CDC of soil water is independent on soil type, the impact of soil mineralogy on the moist-soil dielectric spectra was introduced in [1]–[3] by modifying the CDC dependence on the volumetric soil moisture with the use of specific regression parameters dependent on clay and sand percentages. As a result, with the Debye relaxation parameters for the water located out of soil and the granulometric soil parameters being easily available, the SMDM has appeared to become a universally recognized model in radio thermal and radar remote sensing techniques. Although the SMDM has been derived using only an ensemble consisting of five prototypal soils, neither the error of its predictions in respect to the soils, falling beyond this ensemble of prototypal soils, has so far been properly considered in the literature nor has any analysis of the SMDM error been conducted in comparison with alternative dielectric models.

In this paper, the SMDM prediction error in regard to both the soils used for their development and other soils, whose dielectric data have not been involved in the process of its elaboration, was analyzed. Furthermore, the error of dielectric predictions obtained with the SMDM was compared with that of the generalized refractive mixing dielectric model (GRMDM) developed in [4] and [5]. The latter employs the refractive mixing dielectric model (RMDM) suggested in [6] and upgraded in [7]. In comparison with [6], the RMDM was modified in [7] so as to distinguish between two types of soil water (bound and free), with their CDCs and volumetric moistures being separately determined from dielectric measurements conducted with moist-soil samples. Earlier, the substantial impact of bound water on moist-soil CDC was proved in [8], using another mixing dielectric model. What distinguishes the results of [7] from those of [8] is application of CDCs related to both the bound and free types of soil water, while only the CDC of free water was employed in [8].

Based on the results of [7], in [4] and [5], microwave dielectric spectra of both bound and free types of soil water were shown to follow the Debye relaxation formulas, with the methodology of obtaining the Debye relaxation parameters and ohmic conductivities being devised. Using the GRMDM, the dielectric spectra of moist soils can be predicted [4], [5], [9] for a given type of soil as a function of dry-soil CDC, volumetric moisture, maximum bound water fraction (MBWF), low- and high-frequency limits of dielectric constant (DC), relaxation times, and ohmic conductivities, related to both types of soil water. All these variables were identified [4], [5] as the GRMDM spectroscopic parameters, which depend not only on soil type but also on temperature. As a result, the GRMDM made possible to study the moist-soil CDC spectra dependence on soil type and temperature through the respective dependences of the spectroscopic parameters [10]–[15].

The GRMDM proved to adequately predict the CDC for a given type of moist soil, provided that all the GRMDM spectroscopic parameters are obtained through rather laborious dielectric measurements carried out for each specific soil type (see [4], [5], [7], and [9]–[15]). From this point of view, the

Manuscript received July 20, 2007; revised June 14, 2008 and October 5, 2008. First published April 28, 2009; current version published June 19, 2009. This work was supported in part by the Siberian Branch, Russian Academy of Sciences, under Project 70, by the U.S. Civil Research and Development Foundation under Grant RUG2-2800-KR-06, and by the Russian Foundation for Basic Research under Grant 07-05-96804-r-yenisei-a.

The authors are with the L.V. Kirensky Institute of Physics, Siberian Branch, Russian Academy of Sciences, 660036 Krasnoyarsk, Russia (e-mail: rsdvm@ksc.krasn.ru; rsdvk@ksc.krasn.ru; rsd@ksc.krasn.ru).

Digital Object Identifier 10.1109/TGRS.2008.2011631

GRMDM is less convenient in practical application as compared with the SMDM, which can generate dielectric predictions, with its input parameters being soil granulometric data only. Therefore, the advantage of using the GRMDM instead of the SMDM could be justified if only the accuracy of SMDM dielectric predictions appears to be insufficient, with the latter being the case mentioned in the literature for some soils [16].

Using the dielectric spectra data set measured in [1], [17], and [18], a comparative analysis of the dielectric prediction error related to both the SMDM and GRMDM is carried out. In terms of granulometric mineralogy, the data set from [17] included a broad variety of 11 soil types. The dielectric data employed from [17] concern a wide frequency range (from 45 MHz to 26.5 GHz) at the temperature of 20 °C, with volumetric moistures varying from residual quantities contained in dry soils to values corresponding to field capacity moistures, while the data available from [1] and [18] included measurements in the frequency range from 1.4 to 18 GHz conducted for four soils at the temperature range from 20 °C to 22 °C.

In Sections II and III, the SMDM concept is outlined, and its predictions are correlated with, first, the DC and loss factors (LFs) measured in [1] and [18], which have been used for developing the SMDM, and with, second, the dielectric data measured in [17], with the latter being independent in regard to the SMDM. This analysis revealed good agreement between the SMDM predictions and the data measured in [1] and [18]. At the same time, the SMDM predictions appeared to significantly deviate from the dielectric data measured in [17]. In this case, the predicted LFs were noticed to turn even negative, which contradicts to the physical sense of that quantity. This result challenged us to test an alternative dielectric model, namely, the GRMDM, over the sets of soils measured in [1], [17], and [18]. In Sections IV and V, the GRMDM concept is outlined, and its spectroscopic parameters are derived through regression analysis, using the dielectric data of [1], [17], and [18]. Furthermore, the GRMDM predictions were correlated with the measured dielectric data, revealing the error of prediction to be on the same order as that observed in the case of predicting the data measured in [1] and [18] with the use of the SMDM. In Section VI, based on good correlation between the GRMDM predictions and the measured dielectric data, some regression analysis formulas were fitted to the GRMDM spectroscopic parameters derived for the whole variety of soil types available in [1], [17], and [18], with the values of clay percentage being an independent variable. As a result, regression dependences were obtained for the GRMDM spectroscopic parameters as functions of clay percentage, giving rise to a new dielectric model that is capable to generate dielectric predictions with the use of soil granulometric data, as the SMDM is. This model was named the mineralogy-based soil dielectric model (MBSDM). Furthermore, the MBSDM was tested over the composite dielectric data set borrowed from [1], [17], and [18], which were used for its development. This test proved the MBSDM capability to generate predictions with even smaller error than the SMDM ensures in the case of the soils of [1] and [18], whose dielectric data have been used for its development. At the same time, as shown in Section II, the SMDM revealed substantially greater prediction error when being tested over the dielectric data of [17], which are independent on the data used for developing this model.

Taking into consideration the fact that the SMDM revealed substantially greater prediction error when being tested over the dielectric data of [17], which are independent on the data used for developing this model, in Section VII, there were two versions of the MBSDM produced based on the dielectric data of either [17], or [1], [18]. These versions were then tested over the dielectric data of the soils measured separately in either [1], [18], or [17], thus ensuring the same conditions of testing on independent dielectric data as was the case in Section II in respect to the SMDM. Both versions of the MBSDM demonstrated substantially smaller prediction error in comparison with the SMDM. In addition, in Section VII, the capability of the MBSDM to generate dielectric predictions for an individual soil was analyzed, provided that its version has been developed on the dielectric data of the set of soils, which this specific soil does not belong to.

II. SMDM Concept

The SMDM was developed in [1]–[3] on the bases of dielectric measurements covering five soil types, a wide range of moisture conditions, and two frequency ranges extending from 0.3 to 1.3 GHz (see [2] and [3]) and from 1.4 to 18 GHz (see [1] and [18]). The SMDM has the following form:

$$\varepsilon'_m = \left[1 + \frac{\rho_b}{\rho_s}\left(\varepsilon_s'^{\alpha} - 1\right) + m_v^{\beta'}\varepsilon_{\rm fw}'^{\alpha} - m_v\right]^{1/\alpha} \quad (1)$$

$$\varepsilon''_m = \left[m_\nu^{\beta''}\varepsilon_{fw}''^{\alpha}\right]^{1/\alpha} \quad (2)$$

where ε'_m and ε''_m are the DC and LF of the moist soil, respectively, ε'_s is a composite DC of the soil mineral contents, m_v is the volumetric moisture content, ρ_b is the bulk density in grams per cubic centimeter, ρ_s is the specific gravity of the solid soil particles, $\alpha = 0.65$ is an empirically determined constant, and β' and β'' are the empirically determined soil-type-dependent constants given by

$$\beta' = 1.2748 - 0.00519\,S - 0.00152\,C \quad (3)$$

$$\beta'' = 1.33797 - 0.00603\,S - 0.00166\,C \quad (4)$$

where S and C represent the percentages of sand and clay, respectively. The correlation between the specific gravity, ρ_s, and DC, ε'_s, and the one between the soil bulk density, ρ_b, and dry-soil DC, ε'_{m0}, are given by

$$\begin{aligned}\varepsilon'_s &= (1.01 + 0.44\,\rho_s)^2 - 0.062\\ \rho_b &= \left[(\varepsilon'_{m0})^{\alpha} - 1\right]\rho_s/\left(\varepsilon_s'^{\alpha} - 1\right).\end{aligned} \quad (5)$$

The formulas in (5) are sufficient to determine the dry-soil DC in (1), provided that the following pairs of soil parameters are known: (ρ_b, ρ_s), $(\varepsilon'_{m0}, \rho_s)$, (ρ_b, ε'_s), and $(\varepsilon'_{m0}, \varepsilon'_s)$. Such alternatives can help when analyzing the dielectric data borrowed from the literature. The quantities $\varepsilon'_{\rm fw}$ and $\varepsilon''_{\rm fw}$ are the DC and LF of free water, respectively, given by the Debye equations, with the latter being modified to include a term that accounts for the effective conductivity of the free soil water (FSW)

$$\varepsilon'_{\rm fw} = \varepsilon_{w\infty} + \frac{\varepsilon_{w0} - \varepsilon_{w\infty}}{1 + (2\pi f\tau_w)^2} \quad (6)$$

$$\varepsilon''_{\rm fw} = \frac{2\pi f\tau_w(\varepsilon_{w0} - \varepsilon_{w\infty})}{1 + (2\pi f\tau_w)^2} + \frac{\sigma_{\rm eff}}{2\pi\varepsilon_0 f}\,\frac{(\rho_s - \rho_b)}{\rho_s m_v} \quad (7)$$

where ε_0 is the DC of free space, which is equal to 8.854×10^{-12} F/m, τ_w is the relaxation time for free water, f is the frequency in hertz, ε_{w0} is the low-frequency limit of DC for water, and $\varepsilon_{w\infty} = 4.9$ is the high-frequency limit of $\varepsilon'_{\mathrm{fw}}$. Expressions for τ_w and ε_{w0} are given as functions of temperature by Ulaby *et al.* [19]. At room temperature (20 °C), $2\pi\tau_w = 0.58 \times 10^{-10}$ s and $\varepsilon_{w0} = 80.1$. The effective conductivity σ_{eff} was determined in the following form:

$$\sigma_{\mathrm{eff}} = -1.645 + 1.939\,\rho_b - 0.0225622\,S + 0.01594\,C. \quad (8)$$

According to [1], (1)–(8) must be applied in the frequency range from 1.4 to 18 GHz. For the frequency range from 0.3 to 1.3 GHz considered in [2] and [3], (8) must be substituted by the following expression:

$$\sigma_{\mathrm{eff}} = 0.0467 + 0.2204\,\rho_b - 0.004111\,S - 0.006614\,C. \quad (9)$$

In addition, the DCs of moist soil in the range from 0.3 to 1.3 GHz, ε'_{mlf}, are to be calculated using

$$\varepsilon'_{\mathrm{mlf}} = 1.15\varepsilon'_m - 0.68 \quad (10)$$

where ε'_m is given by (1).

As can be seen in (1)–(10), the dielectric spectrum for a given type of moist soil can be determined via a set of the following parameters:

1) the two values from the following four parameters: the specific gravity of the solid soil particles, ρ_s, the DC, ε'_{m0}, and bulk density, ρ_b, regarding the dry soil, and the composite DC of the soil mineral contents, ε'_s;
2) the volumetric moisture, m_v;
3) the low-frequency limit of DC, $\varepsilon_{\mathrm{fw}}$, of free water;
4) the relaxation time, τ_w, of free water;
5) the mass percentages of sand and clay in the soil, S and C, respectively.

In the following section, the error of the predictions generated with the use of the SMDM will be analyzed in regard to the dielectric data measured in [1], [17], and [18].

III. Error of SMDM Dielectric Predictions

The error of SMDM dielectric predictions was analyzed on the basis of the soils measured in [1], [17], and [18]. The names and physical characteristics for 15 soils are shown in Table I in ascending order of their clay percentages. Only those soils from [1], [17], and [18] which have sufficient dielectric data to carry out our analysis were included in Table I. Codes from A to L and from F1* to F5* correspond to the set of soils measured in [17] and the ensemble of soils named as fields 1, 2, 3, and 5 in [1] and [18], respectively. According to Section I, the data shown in Table I, being complemented with the values of DC for dry soils, which are available in [1], [17], and [18], are sufficient for predicting the DCs and LFs of moist soils with the use of the SMDM. The value of dry-soil DC, ε'_{m0}, related to the soils of [1], [17], and [18] appeared to be on the average of 2.5, as estimated from the dielectric data given in these sources, with little information available to reliably determine its variations that are dependent on soil type.

First, the error of SMDM predictions regarding the soils was estimated, whose dielectric data have been used for the development of the model. In Fig. 1, the measured DCs and LFs are shown as functions of their SMDM predictions in the case of soils measured in [1] and [18], i.e., soils F1*, F2*, F3*, and F5*, according to Table I. The results shown in Fig. 1 are related to the frequency range from 1.4 to 18 GHz. These data were linearly fitted, and the correlation coefficient, standard deviation, and equations of fitting straight lines, which characterize the SMDM prediction error, were estimated. All these statistical characteristics are given in the caption of Fig. 1. In this case, the SMDM was found to provide dielectric prediction, with correlation coefficients being 0.99 and 0.97 for the DC and LF data, respectively. Standard deviations appeared to be 0.88 and 0.55, while the equations of fitting straight lines for the DC and LF are $\varepsilon'_m = -0.934 + 1.08\ \varepsilon'_p$ and $\varepsilon''_m = 0.255 + 1.065\ \varepsilon''_p$, respectively, which quantitatively characterize a noticeable squint of the fitting straight line from the bisectors $\varepsilon'_m = \varepsilon'_p$ and $\varepsilon''_m = \varepsilon''_p$. In the consideration to follow, we will take these values characterizing the error of SMDM predictions as the reference quantities to compare the other dielectric models analyzed. In Fig. 1, the SMDM predictions were tested regarding the soils, whose dielectric data have been used for the development of the model. As a next step, we will test this model with the dielectric data from [17], which can be considered as independent ones in respect to the version of the SMDM applied for calculations.

TABLE I
PHYSICAL AND MINERALOGICAL CHARACTERISTICS OF SOIL SAMPLES

№	Sample	Description (Unified Soil Classification System)	Sand % (by weight)	Silt % (by weight)	Clay % (by weight)	Specific Gravity	Specific Surface m^2/g
1	B	Sand (SP), Light Gray	98	2	0	2.62	0.66
2	L	Sand (SP), Brown	99	1	0	2.66	0.31
3	I	Sand (SP), White	100	0	0	2.67	0.03
4	C	Silty Sand (SM), Brown	88	8	4	2.64	3.64
5	E	Clayey Silt (ML), Brown	TR	93	7	2.59	13.89
6	K	Clayey Silt (ML), Brown; Trace of Sand	4	89	7	2.71	12.5
7	F2*	Loam	42	49.5	8.53	2.70	49
8	G	Clayey Sand (SC), Dark Brown	55	32	13	2.66	33.18
9	F1*	Sandy Loam	51.5	35	13.4	2.66	52
10	F3*	Silt Loam	30.6	55.9	13.5	2.59	66
11	D	Silty Sand (SM), Reddish Brown	77	9	14	2.66	15.01
12	H	Clay (CH), Gray	2	64	34	2.74	40.49
13	F5*	Silty Clay	5.02	47.6	47.4	2.56	252
14	J	Silt (ML), White	0	46	54	2.61	9.29
15	A	Clay (CH), Light Gray	2	22	76	2.34	25.97

For the data set relating to the soils measured in [17], the results of such a test are shown in Fig. 2. The experimental dielectric data shown in Fig. 2 correspond to the temperature of 20 °C. According to [1]–[3], the calculations of DCs and LFs were performed over two frequency ranges, i.e., from

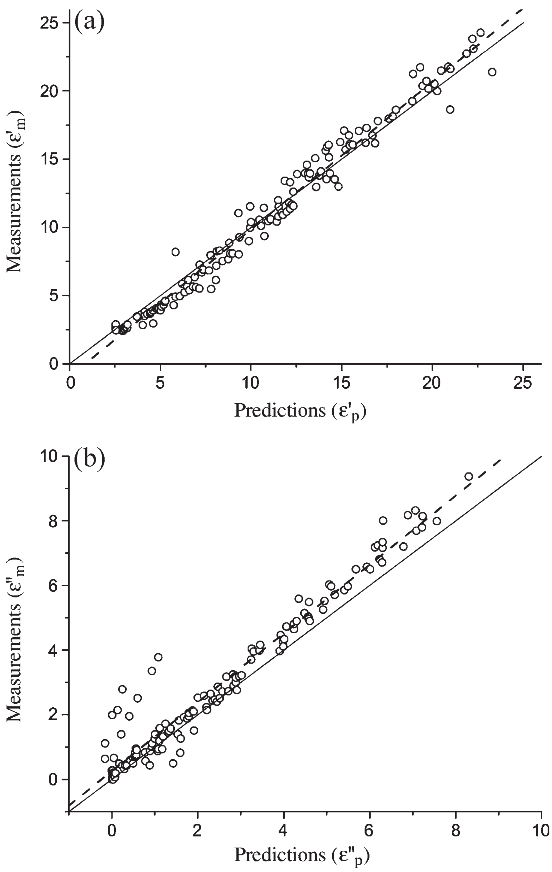

Fig. 1. Correlation of SMDM predictions, ε'_p and ε''_p, for (a) DCs and (b) LFs with the measured ones, ε'_m and ε''_m, in the case of soils measured in [1] and [18]. The solid and dotted lines represent the bisectors and linear fits, respectively. Correlation coefficients, R_{DC} and R_{LF}, and standard deviations, SD_{DC} and SD_{LF}, are equal to $R_{\mathrm{DC}} = 0.99$, $R_{\mathrm{LF}} = 0.974$, $SD_{\mathrm{DC}} = 0.884$, and $SD_{\mathrm{LF}} = 0.55$. The linear fits are expressed as follows: $\varepsilon'_m = -0.934 + 1.08\,\varepsilon'_p$ and $\varepsilon''_m = 0.255 + 1.065\,\varepsilon''_p$.

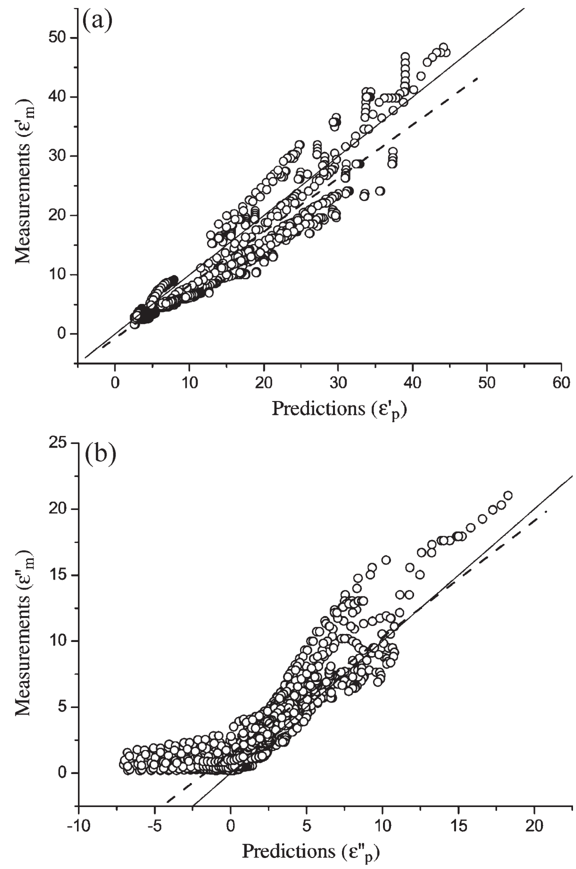

Fig. 2. Correlation of SMDM predictions, ε'_p and ε''_p, for (a) DCs and (b) LFs with the measured ones, ε'_m and ε''_m, in the case of soils measured in [17]. The solid and dotted lines represent the bisectors and linear fits, respectively. Correlation coefficients, R_{DC} and R_{LF}, and standard deviations, SD_{DC} and SD_{LF}, are equal to $R_{\mathrm{DC}} = 0.942$, $R_{\mathrm{LF}} = 0.882$, $SD_{\mathrm{DC}} = 3.391$, and $SD_{\mathrm{LF}} = 1.695$. The linear fits are expressed as follows: $\varepsilon'_m = -0.753 + 0.902\,\varepsilon'_p$ and $\varepsilon''_m = 1.483 + 0.881\,\varepsilon''_p$.

300 MHz to 1.3 GHz and from 1.4 to 21 GHz, using (1)–(7), (9), (10), and (1)–(8), respectively. As seen in Fig. 2, the measured and predicted values shown in Fig. 2 exhibit less correlation coefficients ($R = 0.942$ for DCs and $R = 0.882$ for LFs) compared to the data of [1] and [18], which are shown in Fig. 1. In addition, the predictions in Fig. 2 have a much greater bias compared to that in Fig. 1, with their linear fits being expressed by the following equations: $\varepsilon'_m = -0.753 + 0.902\ \varepsilon'_p$ and $\varepsilon''_m = 1.483 + 0.881\ \varepsilon''_p$ instead of $\varepsilon'_m = \varepsilon'_p$ and $\varepsilon''_m = \varepsilon''_p$. Here, it is worth noting that, as seen in Fig. 2(b), the linear fits used are not the best kinds of fits to be applied in this case, as the data measured distinctly demonstrate nonlinear statistical dependence on the predicted ones. The reason for using linear fits is that the major purpose of our regression analysis is to obtain not the best fit error but the error of linear fits in particular, which give the error of dielectric predictions relative to the rigorous dependences $\varepsilon'_m = \varepsilon'_p$ and $\varepsilon''_m = \varepsilon''_p$. Furthermore, in the frequency range from 1.4 to 5.0 GHz, the LFs predicted were found to become negative, which does not comply with the physical sense of this characteristic.

An illustrative example of quantitative comparison between the predicted and measured spectra for the individual soil coded by D in Table I is shown in Fig. 3, allowing to see how uniformly the SMDM predicts the measured data in a frequency domain. As seen from the results shown in Fig. 3, in case of some moistures, the prediction errors were found to exceed the magnitudes of the measured values themselves.

As a whole, from Figs. 2 and 3, it follows that the SMDM was found to provide substantially larger errors of DC and LF predictions for the soils falling beyond the set of soils used for developing this model. The largest errors in SMDM predictions shown in Fig. 2 cannot be attributed to specific soil types only. These occur for every soil type within a respective frequency range, thus revealing the fact that the SMDM does not uniformly model the dielectric spectra in the whole frequency band, which is clearly seen in Fig. 3. With this result of the SMDM tests, the search for an alternative model that is capable to provide dielectric predictions with respect to the soils, whose dielectric data have not been used for its development, seems to be justified. Taking into account the good predictive power of the GRMDM relative to the individual soil types demonstrated in [4], [5], and [9]–[15], we will consider the possibility of carrying out such a search on the basis of the GRMDM as a building block. In Sections IV and V, the concept of the GRMDM will be outlined, and the same correlation analysis will be conducted regarding the capability of the GRMDM to make accurate predictions in the whole domain of moistures,

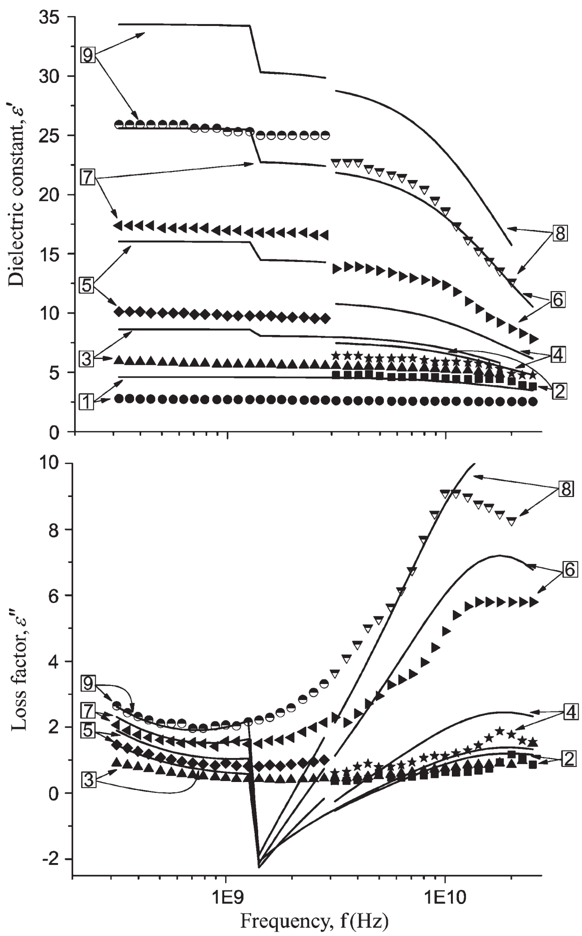

Fig. 3. DC and LF spectra (dots) measured and (solid lines) predicted with the use of the SMDM in the case of soil D (see Table I). The shown data correspond to the following soil volumetric moistures m_v(%): (1) 3.2, (2) 8, (3) 8.8, (4) 13.2, (5) 18.4, (6) 29.1, (7) 29.7, (8) 38.2, and (9) 39.4.

frequencies, and granulometric mineralogy characteristics for the sets of soils measured in [1], [17], and [18].

IV. GRMDM CONCEPT

In contrast to the SMDM, exclusively employing the dielectric spectrum valid for the water located out of the soil, the GRMDM employs the spectra explicitly related to either bound soil water (BSW) or FSW. The description of this model is given in the following.

In accordance with [5] and [6], the DC, ε'_m, and LF, ε''_m, as functions of volumetric moisture W can be represented in the form of the RMDM

$$\varepsilon'_m = n_m^2 - \kappa_m^2 \quad \varepsilon''_m = 2n_m\kappa_m \tag{11}$$

$$n_m = \begin{cases} n_d+(n_b-1)m_v, & m_v \le m_{vt} \\ n_d+(n_b-1)m_{vt}+(n_u-1)(m_v-m_{vt}), & m_v \ge m_{vt} \end{cases} \tag{12}$$

$$\kappa_m = \begin{cases} \kappa_d + \kappa_b m_v, & m_v \le m_{vt} \\ \kappa_d + \kappa_b m_{vt} + \kappa_u(m_v - m_{vt}), & m_v \ge m_{vt} \end{cases} \tag{13}$$

where n_m, n_d, n_b, n_u, and κ_{m}, κ_{d}, κ_{b}, κ_{u} are the values of refractive index (RI) and normalized attenuation coefficient (NAC), which is understood here as a proportion of the standard attenuation coefficient to the free-space propagation constant.

The subscripts m, d, b, and u in (11)–(13) stand for moist soil, dry soil, BSW, and FSW, respectively, and m_{vt} is a value of the MBWF in a given type of the soil. The latter depends on the soil mineral contents [9]. The values of RI and NAC, relating to dry soil and BSW or FSW, can be written through respective DCs and LFs with the use of

$$n_{d,b,u}\sqrt{2} = \sqrt{\sqrt{\left(\varepsilon'_{d,b,u}\right)^2 + \left(\varepsilon''_{d,b,u}\right)^2} + \varepsilon'_{d,b,u}} \tag{14}$$

$$\kappa_{d,b,u}\sqrt{2} = \sqrt{\sqrt{\left(\varepsilon'_{d,b,u}\right)^2 + \left(\varepsilon''_{d,b,u}\right)^2} - \varepsilon'_{d,b,u}} \tag{15}$$

where the DC and LF for bound and free water components are presented, respectively, with the Debye relaxation equations

$$\varepsilon'_{b,u} = \varepsilon_\infty + \frac{\varepsilon_{0b,0u} - \varepsilon_\infty}{1 + (2\pi f\tau_{b,u})^2},$$
$$\varepsilon''_{b,u} = \frac{\varepsilon_{0b,0u} - \varepsilon_\infty}{1 + (2\pi f\tau_{b,u})^2} 2\pi f\tau_{b,u} + \frac{\sigma_{b,u}}{2\pi\varepsilon_0 f}. \tag{16}$$

In the formulas of (16), the value f denotes the wave frequency, while the values $\sigma_{b,u}$, $\tau_{b,u}$, and $\varepsilon_{0b,0u}$ are the conductivities, relaxation times, and low-frequency limit of DCs, respectively, relating to either BSW or FSW components. The value ε_0 is the DC for free space, while ε_∞ represents the DC in the high-frequency limit, which is equal to 4.9 for both the bound and free types of soil water. As can be seen from (11)–(16), a certain type of moist soil, in terms of its dielectric spectra, can be completely determined via a set of the following spectroscopic parameters:

1) DC, ε'_d, for dry soil;
2) LF, ε''_d, for dry soil;
3) value of the MBWF, m_{vt};
4) low-frequency limits of DCs, ε_{0b} and ε_{0u}, for BSW and FSW;
5) relaxation times, τ_b and τ_u, for BSW and FSW;
6) conductivities, σ_b and σ_u, for BSW and FSW.

For a specific type of soil, all of these parameters can be derived with the use of conventional dielectric measurements regarding moist soils, as given in [4], [5], and [10]. Therefore, for it to be employed in microwave remote sensing processing algorithms, this model requires a set of prior dielectric measurements to be carried out for a set of individual soils involved in remote sensing data processing, and the error of dielectric predictions for each individual soil to be tested. In the subsequent paragraph, analysis of GRMDM prediction errors, using the dielectric data of [1], [17], and [18], will be performed.

V. GRMDM PREDICTIONS FOR THE DIELECTRIC SPECTRA

The ensemble of dielectric data in [1], [17], and [18] appeared to be incomplete, in terms of the number of moistures measured, to apply, for deriving the GRMDM spectroscopic parameters, the methodology proposed earlier in [4] and [5], as the latter suggests a procedure of calculating the derivatives

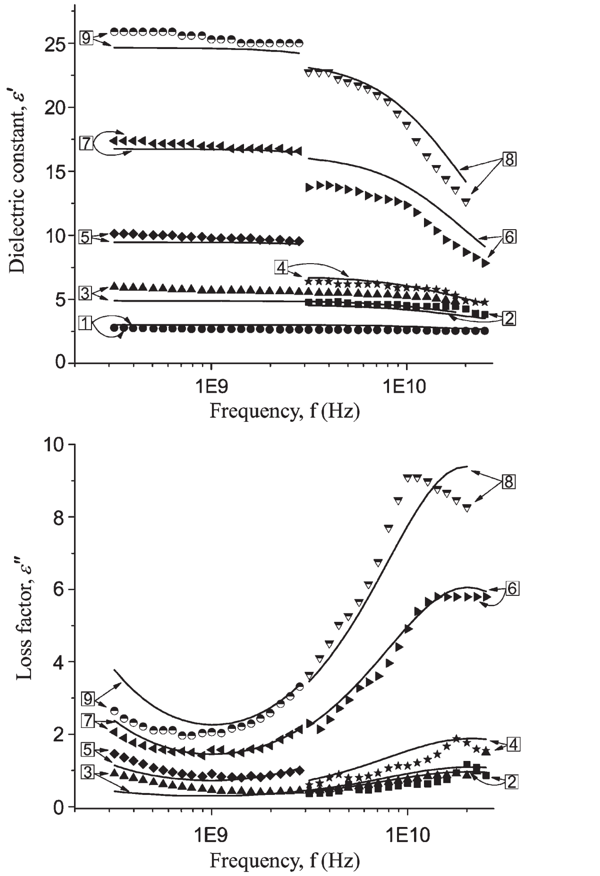

Fig. 4. DC, ε', and LF, ε'', spectra for soil D (dots) measured and (solid line) fitted with the use of the GRMDM model. The shown data correspond to the following soil volumetric moistures $m_v(\%)$: (1) 3.2, (2) 8, (3) 8.8, (4) 13.2, (5) 18.4, (6) 29.1, (7) 29.7, (8) 38.2, and (9) 39.4.

by volumetric moisture from the RIs and NACs measured as functions of volumetric moisture. Therefore, a procedure of fitting simultaneously (11)–(16) to all the DC and LF spectra corresponding to the whole set of moistures available for each particular type of soils presented in Table I was applied. The OriginPro 7.5 product was employed to perform such a multiple-data fitting. At the first stage of fitting, spectra with smaller values of moisture were used, with the soil water presumably consisting of only bound molecules, which corresponds to the range of moistures $m_v < m_{vt}$. At the second stage of multiple-data fitting, the dielectric data employed at the first stage were complemented with the data related to the rest of soil moistures available to finally derive the value of MBWF and free-water conductivity. As shown in [9], the low-frequency limit of DC and relaxation time, relating to FSW, appeared to be the functions only slightly varying with soil mineralogy. Therefore, in the second stage of fitting, these values were assigned to be equal to statistical averages, $\varepsilon_{0u} = 100$ and $\tau_u = 8.5$ ps, defined on the basis of data available in [9]. As an example of fitting procedure, in the case of soil D, the fitting graphs and the experimental spectra being fitted are shown in Fig. 4. The GRMDM allows to individually adjust its input parameters to each specific type of soil. As a result, the spectra predicted in Fig. 4 appeared to be a lot closer to the experimental spectra than those shown in Fig. 3, which are calculated with the SMDM.

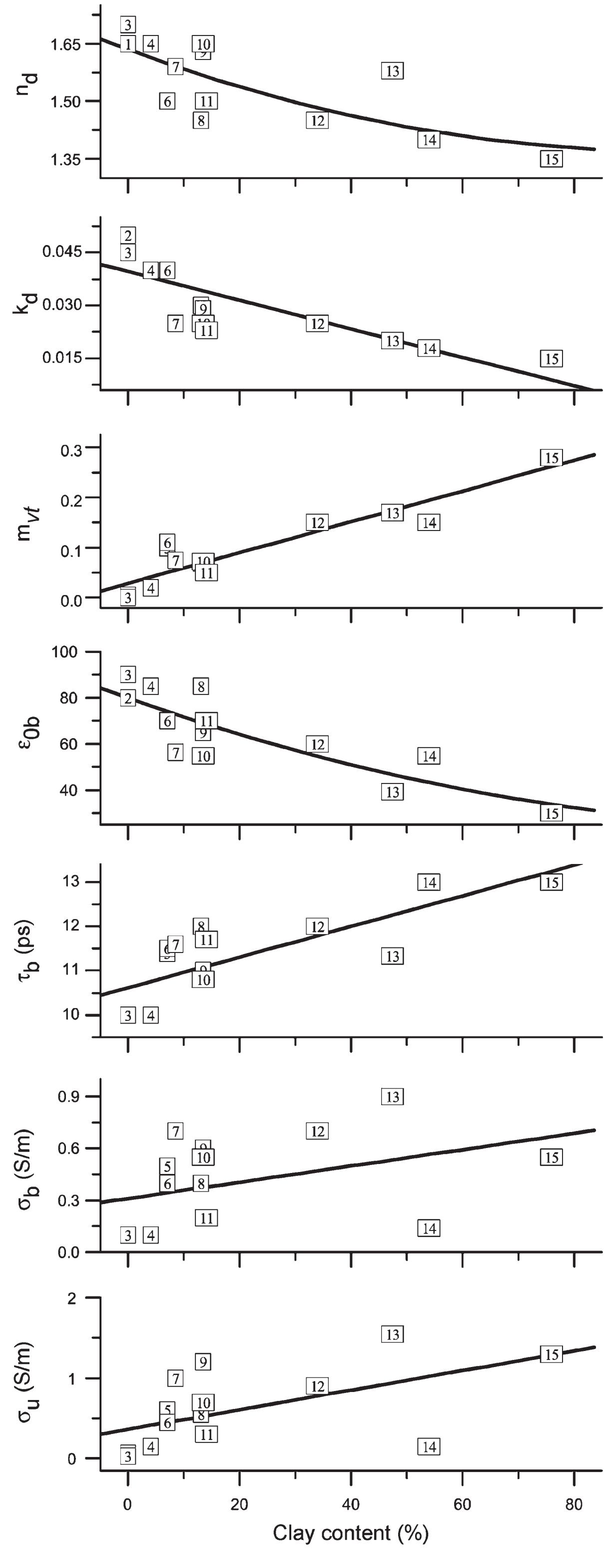

Fig. 5. GRMDM spectroscopic parameters for the soils presented in Table I as functions of granulometric clay content. The squares represent the values derived through fitting the dielectric spectra. The numbers shown in squares correspond to those given in Table I.

The GRMDM spectroscopic parameters obtained with this technique are shown in Fig. 5 as functions of clay content. To compare the error of GRMDM predictions with those related to the SMDM, the GRMDM predictions were calculated for

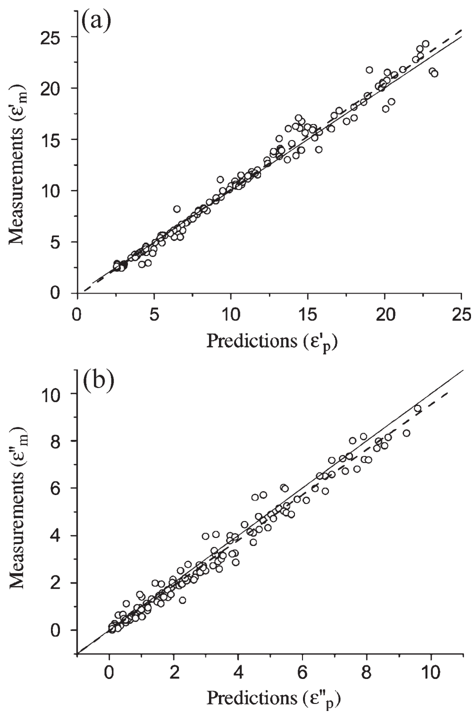

Fig. 6. Correlation of GRMDM predictions, ε'_p and ε''_p, for (a) DCs and (b) LFs with the measured ones, ε'_m and ε''_m, in the case of soils measured in [1] and [18]. The solid and dotted lines represent the bisectors and linear fits, respectively. Correlation coefficients, R_{DC} and R_{LF}, and standard deviations, SD_{DC} and SD_{LF}, are equal to $R_{\mathrm{DC}} = 0.992$, $R_{\mathrm{LF}} = 0.989$, $SD_{\mathrm{DC}} = 0.791$, and $SD_{\mathrm{LF}} = 0.3637$. The linear fits are expressed as follows: $\varepsilon'_m = -0.2309 + 1.034\,\varepsilon'_p$ and $\varepsilon''_m = 0.3063 + 0.957\,\varepsilon''_p$.

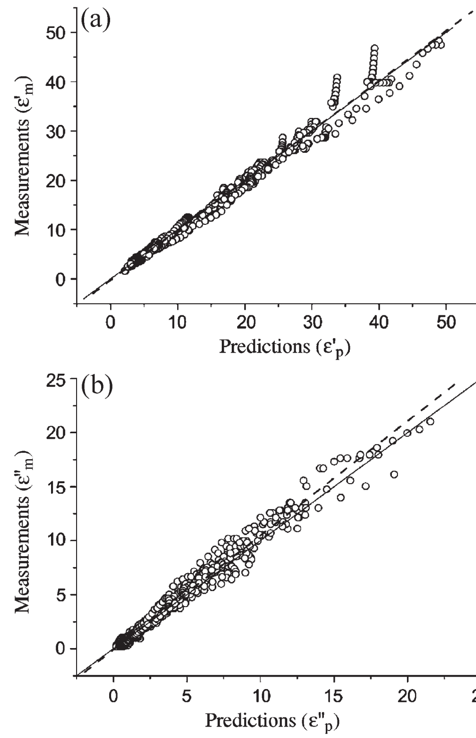

Fig. 7. Correlation of GRMDM predictions, ε'_p and ε''_p, for (a) DCs and (b) LFs with the measured ones, ε'_m and ε''_m, in the case of soils measured in [17]. The solid and dotted lines represent the bisectors and linear fits, respectively. Correlation coefficients, R_{DC} and R_{LF}, and standard deviations, SD_{DC} and SD_{LF}, are equal to $R_{\mathrm{DC}} = 0.995$, $R_{\mathrm{LF}} = 0.991$, $SD_{\mathrm{DC}} = 1.023$, and $SD_{\mathrm{LF}} = 0.4899$.The linear fits are expressed as follows: $\varepsilon'_m = -0.2753 + 1.013\,\varepsilon'_p$ and $\varepsilon''_m = -0.0943 + 1.058\,\varepsilon''_p$.

the group of soils shown in Fig. 1, using the spectroscopic parameters given in Fig. 5. The graph presenting the measured dielectric data versus the GRMDM predictions is shown in Fig. 6. As follows from comparing the results shown in Figs. 1 and 6 for the SMDM and GRMDM, respectively, the errors of predictions, in terms of the correlation coefficient, standard deviation, and the bias of the fitting straight line, are very close to each other. Consequently, with regard to the soils, whose dielectric data were used for developing both the SMDM and GRMDM, these models generate dielectric predictions with about the same error.

Keeping in mind the fact that the mineralogical diversity of the soil measured in [17] is much larger than that of the set of soils measured in [1] and [18] (see Table I and Fig. 5), we will test the GRMDM over the soils of [17]. As seen from Fig. 7 pertaining to soils of [17], the GRMDM provides, in this case, dielectric predictions with the same error as it did in the case of soils of [1] and [18]. Generalizing based on the aforesaid information, it is possible to assert that the GRMDM, having been adjusted to each specific soil, was found to ensure as small error of dielectric predictions for any separate group of soils as the SMDM does, provided that the latter has been adjusted to this particular group.

At the same time, as follows from Figs. 2 and 3, the SMDM predictions related to a group of soils (see Fig. 2) or a specific soil (see Fig. 3) falling beyond the group of soils used for development of the SMDM appeared to have much greater error of dielectric predictions than that related to the soils used for its development. To some extent, this fact brings into question the capability of the SMDM as a whole to generate dielectric predictions with the error given in [1]–[3], in the case of soil variety broader than that of [1] and [18]. Furthermore, we will consider a possibility to build up the dielectric model based on the GRMDM that generates predictions with the error to be valid for an arbitrary group of soils, other than those initially used for its development. At the same time, this model is expected to provide predictions using the input parameters, in terms of mineralogy, similar to those as the SMDM applies. In order to achieve this goal, the GRMDM spectroscopic parameters shown in Fig. 5 were correlated with the granulometric contents of soils, giving rise to a new MBSDM. In the following section, this model will be developed and tested.

VI. MBSDM Concept and Dielectric Prediction Error

The soil granulometric contents, as seen from Table I, are described with sand, silt, and clay percentages. In fact, only two of these are independent because of the mass conservation equation, Clay% + Sand% + Silt% $= 100\%$. To make a decision on which of the three percentages the GRMDM parameters depend most of all, linear and polynomial 1-D functions were fitted to the measured values shown in Fig. 5, with independent variables being consecutively clay, sand, and silt percentages. The results of this regression proved the GRMDM parameters to be most dependent on clay percentage. The fits with the clay percentage being an independent variable are shown in Fig. 5

with solid lines, while the respective fitting equations are given by the following formulas:

$$n_d = 1.634 - 0.539 \cdot 10^{-2}\, C + 0.2748 \cdot 10^{-4}\, C^2$$

$$R_{nd}^2 = 0.535 \quad SD_{nd} = 0.0821 \tag{17}$$

$$k_d = 0.03952 - 0.04038 \cdot 10^{-2}\, C$$

$$R_{kd} = -0.798 \quad SD_{kd} = 0.00724 \tag{18}$$

$$m_{vt} = 0.02863 + 0.30673 \cdot 10^{-2}\, C$$

$$R_{mvt} = 0.922 \quad SD_{mvt} = 0.03049 \tag{19}$$

$$\varepsilon_{0b} = 79.8 - 85.4 \cdot 10^{-2}\, C + 32.7 \cdot 10^{-4}\, C^2$$

$$R_{\varepsilon 0b}^2 = 0.716 \quad SD_{\varepsilon 0b} = 9.87 \tag{20}$$

$$\tau_b = 1.062 \cdot 10^{-11} + 3.450 \cdot 10^{-12} \cdot 10^{-2}\, C$$

$$R_{\tau b} = 0.785 \quad SD = 6.46 \cdot 10^{-13} \tag{21}$$

$$\sigma_b = 0.3112 + 0.467 \cdot 10^{-2}\, C$$

$$R_{\sigma b} = 0.4039 \quad SD_{\sigma b} = 0.2528 \tag{22}$$

$$\sigma_u = 0.3631 + 1.217 \cdot 10^{-2}\, C$$

$$R_{\sigma u} = 0.562 \quad SD_{\sigma u} = 0.4255 \tag{23}$$

$$\varepsilon_{0u} = 100 \tag{24}$$

$$\tau_u = 8.5 \cdot 10^{-12}. \tag{25}$$

The clay content, C, and relaxation times, τ_b and τ_u, in (17)–(23) are expressed in percentages and seconds, respectively. R_j and SD_j denote the correlation coefficient and standard deviation, respectively, related to a certain GRMDM parameter ($j = n_d$, κ_d, m_{vt}, ε_0, τ_b, σ_b, or σ_u). Furthermore, (17)–(25) will be referred to as the MBSDM fits, while the values calculated with these equations will be called as the MBSDM spectroscopic parameters. Finally, the DCs and LFs calculated with (11)–(25) will be identified as the MBSDM dielectric predictions.

At the same time, in the most preferably applied dielectric models [1], [8], both clay and sand percentages are used as independent variables in the respective regression analyses. Therefore, it is worthwhile to clear up what degree of fitting error improvement can be achieved, regarding (17)–(23), with the use of 2-D fitting functions. For this purpose, fitting of the formula $P_j = A_j + B_{cj}C + B_{sj}S$ to the values of the GRMDM parameters shown in Fig. 5 ($j = n_d$, κ_d, m_{vt}, ε_0, τ_b, σ_b, and σ_u) was performed. In the case of the MBWF, m_{vt}, the results of both 1-D (clay percentage) and 2-D (clay and sand percentages) linear fits are shown in Fig. 8. As seen

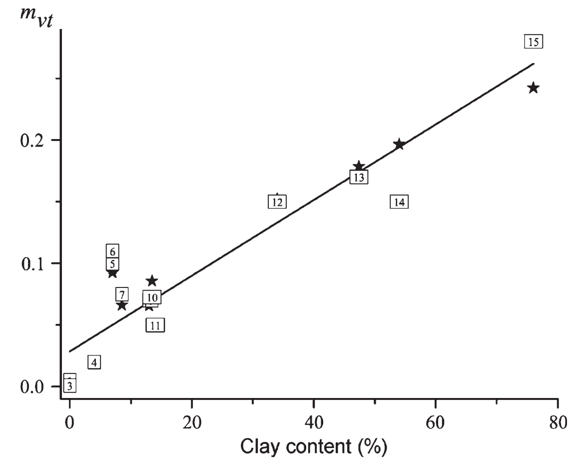

Fig. 8. Fits of formulas $m_{vt} = A + B_cC + B_sS$ (given by asterisks; $A = 0.081$, $B_c = 0215$, $B_s = 0.078$, and $R^2 = 0.94$) and $m_{vt} = A + B_cC$ (given by solid line; $A = 0.029$, $B_c = 0.307$, and $R = 0.92$) to the MBWF, m_{vt}, values shown in Fig. 4. The numbers shown in squares correspond to those assigned for the soils in Table I. Some fitting values, shown as asterisks, are screened with the respective squares.

from Fig. 8, only minor improvement in terms of the correlation coefficient ($R^2 = 0.94$ versus $R = 0.92$) occurred with the introduction of the sand percentage as a second variable. Similar to the case of the MBWF shown in Fig. 8, all the other GRMDM parameters were fitted, proving no significant improvement in their correlation characteristics due to the introduction of the sand percentage as a second variable. Therefore, to allow transfer from the GRMDM to the MBSDM, we will use the 1-D fits (17)–(25) for the GRMDM parameters, with the clay percentage being the only input parameter of the MBSDM in terms of mineralogy, which characterizes a specific type of soil. Furthermore, the effectiveness of the 1-D fits (17)–(25) will be validated by comparing the errors of dielectric predictions obtained with the use of either the GRMDM or MBSDM.

To estimate the correlation between the MBSDM dielectric predictions and the measured DCs and LFs, the experimental DCs and LFs are shown in Fig. 9 versus the predicted ones for the united ensemble of soils presented in [1], [17], and [18]. The correlation analysis shown in Fig. 9 signifies that, over the whole variety of soil types, moistures, and frequencies measured in [1], [17], and [18], the MBSDM is able to predict the DCs and LFs with the same accuracy, in terms of correlation coefficient and standard deviation, as that in the GRMDM (see Figs. 6 and 7). It is also worth noting that this error proved to be on the same order as the SMDM error shown in Fig. 1. This result indirectly justifies the use of the 1-D MBSDM fits given by (17)–(25). The fact that the MBSDM and GRMDM prediction errors were found to be on the same order (compare Fig. 9 with Figs. 6 and 7) should be attributed to a rather good correlation of the most important MBSDM fits with the respective GRMDM spectroscopic parameters, on which dielectric predictions must depend most of all. As follows from the fits given by (17)–(23), these are MBWF, m_{vt}, low-frequency limit of DC, ε_{0b}, and relaxation time, τ_b, for BSW. In spite of the fact that the rest of the MBSDM fits in (17)–(23) did not exhibit substantial correlation with the GRMDM spectroscopic parameters, their impact on the MBSDM dielectric predictions appeared to be of

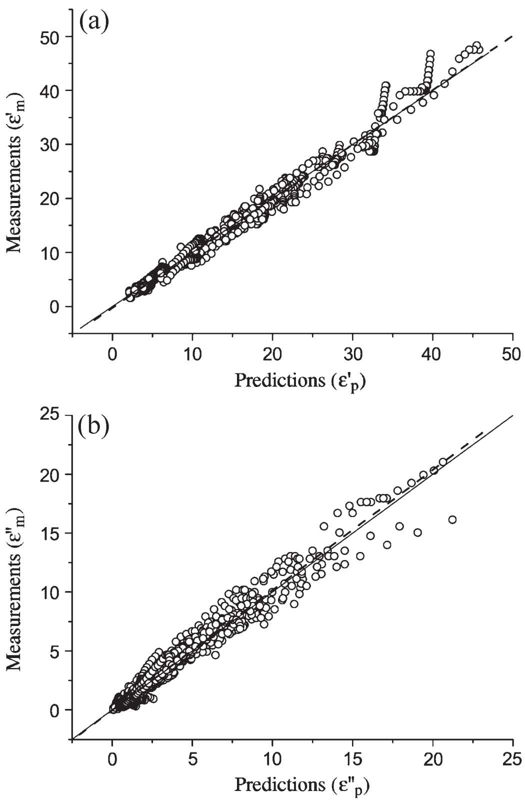

Fig. 9. Correlation of MBSDM predictions, ε'_p and ε''_p, for (a) DCs and (b) LFs with the measured ones, ε'_m and ε''_m, in the case of the consolidated ensemble of soils studied in [1], [17], and [18]. The solid and dotted lines represent the bisectors and linear fits, respectively. Correlation coefficients, R_{DC} and R_{LF}, and standard deviations, SD_{DC} and SD_{LF}, are equal to $R_{\mathrm{DC}} = 0.992$, $R_{\mathrm{LF}} = 0.983$, $SD_{\mathrm{DC}} = 1.259$, and $SD_{\mathrm{LF}} = 0.64$. The linear fits are expressed as follows: $\varepsilon'_m = -0.216 + 1.007\ \varepsilon'_p$ and $\varepsilon''_m = -0.01765 + 1.019\ \varepsilon''_p$.

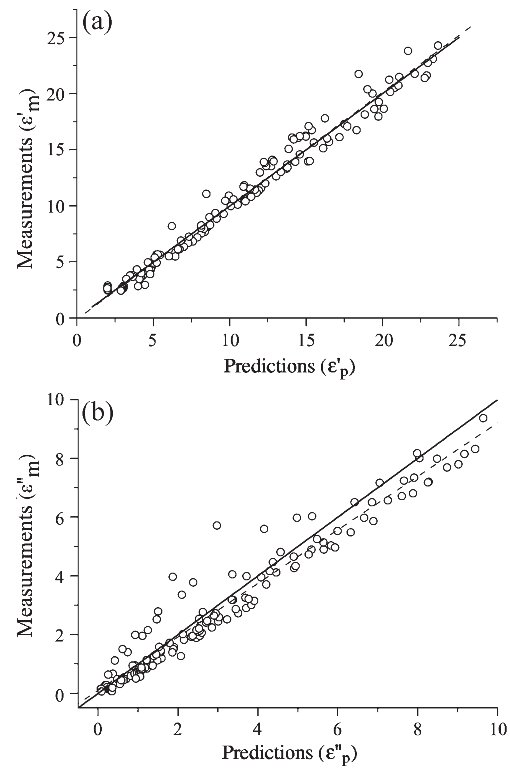

Fig. 10. Correlation of MBSDM predictions, ε'_p and ε''_p, for (a) DCs and (b) LFs with the measured ones, ε'_m and ε''_m, in the case of soils studied in [1] and [18]. The MBSDM version is based on the dielectric data from [17]. The solid and dotted lines represent the bisectors and linear fits, respectively. Correlation coefficients, R_{DC} and R_{LF}, and standard deviations, SD_{DC} and SD_{LF}, are equal to $R_{\mathrm{DC}} = 0.99$, $R_{\mathrm{LF}} = 0.97$, $SD_{\mathrm{DC}} = 0.88$, and $SD_{\mathrm{LF}} = 0.57$. The linear fits are expressed as follows: $\varepsilon'_m = -0.106 + 1.01\ \varepsilon'_p$ and $\varepsilon''_m = 0.101 + 0.911\ \varepsilon''_p$.

minor degree only. Indeed, the respective error characteristics shown in Figs. 6, 7, and 9 related to the GRMDM and MBSDM, respectively, are really close to each other. As a result, with clay percentage being the only mineralogical parameter, the MBSDM proved to be a spectroscopic dielectric model that is capable to predict the CDCs of moist soils with the error on the same order as that related to the GRMDM. Consequently, the MBSDM retained the accuracy of the GRMDM, complementing this feature with the simplicity of its application, which is as simple as that of the SMDM. Nevertheless, it is worth mentioning that the MBSDM prediction error has been so far tested (see Fig. 9) over only the dielectric data used for its development.

We have to recall that the SMDM also demonstrated good predictions when being validated over the dielectric data set that has been used to develop this model (see Fig. 1). In case the test is carried out regarding the dielectric data with which a respective regression model is created, it can reveal only an error of regression analysis itself, which appeared to be quite suitable for both the SMDM and MBSDM, while the test pertaining to the SMDM that has been validated, as shown in Fig. 2, revealed a composite error containing both a regression analysis error and the one that characterizes the model's principal ability to provide appropriate dielectric predictions in the case of soils falling beyond a set of those used for its development. As seen from Fig. 2, the composite error was found to be about three times as great as the regression analysis error seen in Fig. 1, at least in terms of standard deviation. From this point of view, the prediction error of the MBSDM shown in Fig. 9 must be considered as the one relating to regression analysis only. In this respect, it is quite similar to the regression error of the SMDM shown in Fig. 1, although being relevant to a lot broader variety of soil mineralogical characteristics (see Table I). Hence, like it was done relative to the SMDM (see Fig. 2), the MBSDM has to be tested over the dielectric data set other than the one used for deriving (17)–(23). Such a test is expected to reveal an intrinsic predictive power of this model. The respective study is outlined in the next section.

VII. Validation of MBSDM Predictions Over Independent Dielectric Data

To perform such a validation of the MBSDM, (17)–(23) were obtained with the use of spectroscopic parameters relating to the soils studied only in [17] or only in [1] and [18]. This yielded two new versions of the MBSDM, which contained the fitting parameters other than those in (17)–(23) and could be treated as independent with respect to the dielectric data from [1] and [18] or from [17]. In Figs. 10 and 11, the MBSDM predictions for the DC and LF, with the respective versions of the MBSDM being based on the independent dielectric data taken sequentially from [17] or [1], [18] are plotted versus the

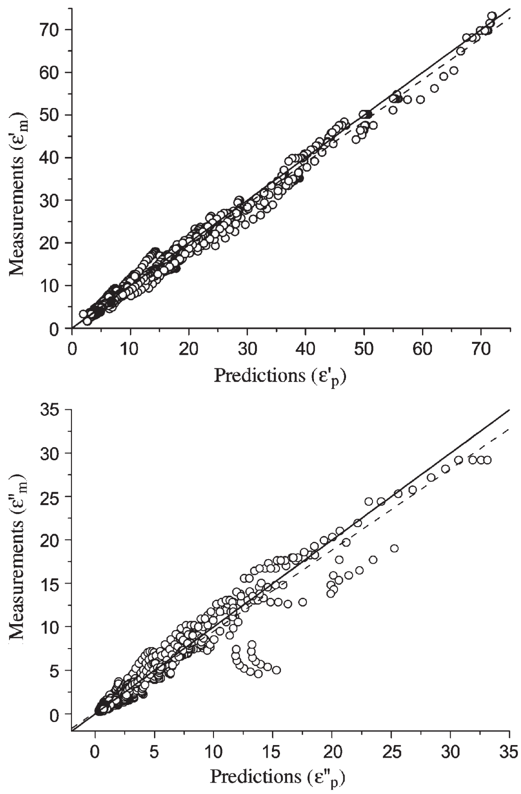

Fig. 11. Correlation of MBSDM predictions, ε'_p and ε''_p, for (a) DCs and (b) LFs with the measured ones, ε'_m and ε''_m, in the case of soils measured in [17]. The MBSDM version is based on the dielectric data from [1] and [18]. The solid and dotted lines represent the bisectors and linear fits, respectively. Correlation coefficients, R_{DC} and R_{LF}, and standard deviations, SD_{DC} and SD_{LF}, are equal to $R_{\mathrm{DC}} = 0.995$, $R_{\mathrm{LF}} = 0.965$, $SD_{\mathrm{DC}} = 1.241$, and $SD_{\mathrm{LF}} = 1.23$. The linear fits are expressed as follows: $\varepsilon'_m = -0.0275 + 0.972\, \varepsilon'_p$ and $\varepsilon''_m = 0.1902 + 0.932\, \varepsilon''_p$.

initially measured data taken in reverse order, i.e., from [1], [18] or [17].

Comparing the results of testing shown in Figs. 9–11, we can see how the MBSDM prediction error power is modified, which is dependent on a dielectric data set used for its development. The least error of prediction was achieved when all the soils were used to develop the MBSDM, with the latter being validated over the same set of soils (see Fig. 9). In this case, the value of error characterizes only a regression analysis error. The greatest error is observed in Fig. 11 when only 4 out of 15 soils were used to develop the respective version of the MBSDM, with their clay content varying from 8.5% to 47%, while the clay content of the soils, whose DC and LF are predicted in Fig. 11, varied from 0% to 76%. Consequently, the MBSDM version used in Fig. 11 was trained on a poorer variety of soils, in terms of mineral contents, than the one for which it generated dielectric predictions. At the same time, the prediction error observed in Fig. 10 is almost the same as that seen in Fig. 9. This situation can be attributed to the fact that the version of the MBSDM used in Fig. 10 was trained on the variety of soil types as broad, in terms of their mineral contents, as the version used in Fig. 9 is. Indeed, the range of clay content, from 0% to 76%, appeared to be the same for both the variety of 11 soils measured in [17] and the variety of 15 soils measured in [1], [17], and [18] (see Table I). At the same time, regarding the data shown in Figs. 2 and 11, it should be noted that the MBSDM used in Fig. 11 was based on a poor variety of soils measured in [1] and [18] as the SMDM was. Nevertheless, this version of the MBSDM provided dielectric predictions over the broader variety of soils [17] with substantially less error (see Fig. 11) compared to the ones generated by the SMDM (see Fig. 2).

It is worth noting here that the methodology employed for developing the MBSDM is based on two key elements. The first one is the GRMDM, which ensures accurate dielectric predictions using a cluster of the GRMDM parameters pertaining to every individual soil type with specific mineral contents, as shown in Figs. 5–7. The second key element is the completeness of an ensemble of such clusters in terms of mineral content diversity of the soils involved. An example of such an ensemble is shown in Fig. 5. Within the MBSDM methodology, the ensemble of the GRMDM parameters pertaining to a specific group of soils is turned into a specific collection of regression equations like (17)–(25), which represent a specific version of the MBSDM related to that group of soils. The broader group of soils, in terms of mineralogical contents, is available; the less error of prediction with the respective version of the MBSDM can be attained, particularly in regard to the soils other than those used to develop the particular version of the MBSDM.

Therefore, the MBSDM prediction error, regarding the whole variety of natural soils, must depend on both the predictive capability of the GRMDM, which is a physically based building block of the MBSDM, and the completeness of the group of soils employed, in terms of diversity of their mineral contents, which is a regression analysis building block of the respective version of the MBSDM. With the use of a more complete data set, the less regression analysis error in equations similar to (17)–(25) can be obtained, thus ensuring less error of predictions related to the respective MBSDM version.

One more problem regarding the MBSDM prediction error needs to be discussed. It concerns the question whether the MBSDM trained on a specific variety of soils is able to provide dielectric spectra predictions in the case of an individual soil, which may belong to or fall out of that variety. The latter is just the case for the SMDM predictions shown in Fig. 2. Let us consider both situations. In Figs. 12 and 13, experimental DCs and LFs are plotted versus the MBSDM predictions in the case of specific soil D measured in [17]. At that, in Figs. 12 and 13, the versions of the MBSDM based on the consolidated group of soils measured in [1], [17], and [18] and on the soils measured only in [1] and [18] were used, respectively.

As seen from Figs. 4 and 12, the error of prediction in the case of an individual soil D, with the MBSDM trained on a composite variety of soils measured in [1], [17], and [18], is almost on the same order as the one obtained individually for this soil with the use of the GRMDM (Fig. 4). The largest deviations are observed in the lower frequency range only for the LF in the case of soils with noticeable amount of free water (graphs 6 and 8), which can be attributed to a rather poor correlation of the MBSDM fit for free-water conductivity with the respective GRMDM parameter values [see Fig. 5 and (23)]. This paper has shown the error of MBSDM predictions for each individual soil from [17] to be on the same order as that seen in Fig. 12. In this respect, Fig. 13 is analogous to Fig. 2, in which the SMDM predictions for soil D of [17] are shown, while the SMDM was trained with the use of dielectric data for the soils

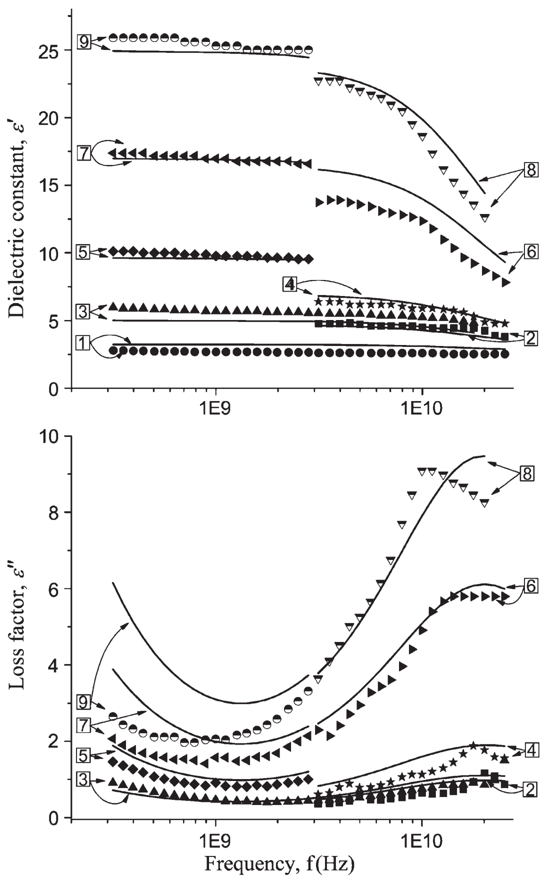

Fig. 12. DC, ε', and LF, ε'', spectra for soil D (dots) measured and (solid line) predicted with the use of the MBSDM trained on the consolidated ensemble of soils of [1], [17], and [18]. The shown data correspond to the following soil volumetric moistures m_v(%): (1) 3.2, (2) 8, (3) 8.8, (4) 13.2, (5) 18.4, (6) 29.1, (7) 29.7, (8) 38.2, and (9) 39.4.

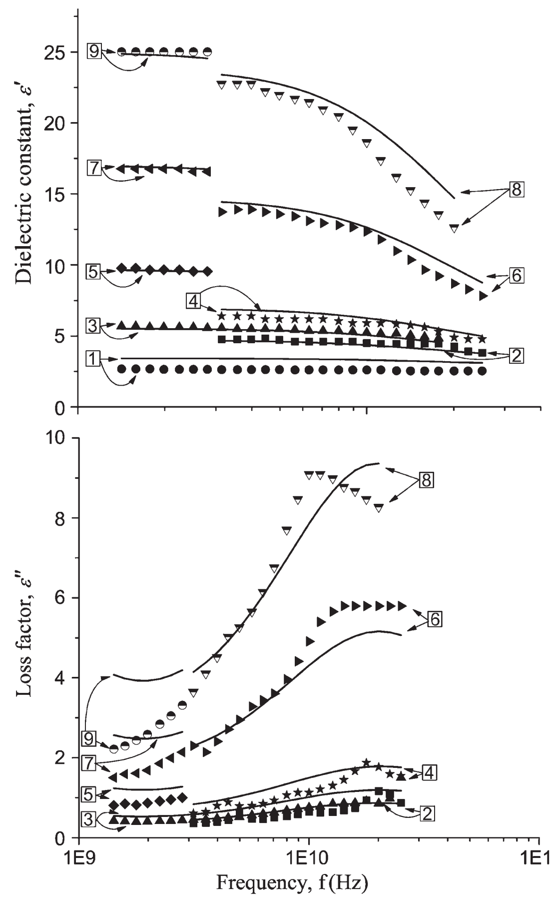

Fig. 13. DC, ε', and LF, ε'', spectra for soil D (dots) measured and (solid line) predicted with the use of the MBSDM trained on the soils of [1] and [18]. The shown data correspond to the following soil volumetric moistures m_v(%): (1) 3.2, (2) 8, (3) 8.8, (4) 13.2, (5) 18.4, (6) 29.1, (7) 29.7, (8) 38.2, and (9) 39.4.

from [1] and [18]. It should be noted that the dielectric data presented in [1] and [18] concern the frequency range from 1.4 to 18 GHz only. In addition, the original dielectric data used to develop the SMDM in the frequency range from 0.3 to 1.3 GHz are not presented in [2] to the extent that is sufficient enough to develop the MBSDM effectively over this range. Therefore, the frequencies shown in Fig. 13 are limited within the frequency range from 1.4 to 18 GHz. As seen from Figs. 2 and 13, the MBSDM provided much more accurate predictions of the DCs and LFs relating to an individual soil D than the SMDM did, with both models having been trained on the same variety of soils. As a result, it can be stated that the MBSDM has demonstrated noticeably less prediction error, compared to the SMDM, in the case of a group of soils or an individual soil falling out of the varieties of soils used to develop the respective models.

VIII. Conclusion

Summing up the results, the following has to be stated as the primary findings of this paper. First, the GRMDM, recently developed in [4] and [5], confirmed its ability to generate dielectric predictions over the ensemble consisting of 15 natural soils having a wide variety of mineralogy contents. These predictions proved to be accurate, concerning the frequency range from 0.3 to 26.5 GHz and volumetric moistures spanning from nearly dry condition to field capacity moistures, with temperatures being from 20 °C to 22 °C.

Second, with the use of spectroscopic parameters of the GRMDM for 15 natural soils, the MBSDM was developed, the only input parameter of which is the content of clay in the soil. This model was shown to generate as good dielectric predictions as the GRMDM does.

Third, it can be stated that the proposed MBSDM proved to generate the predictions of the CDC spectra of moist soils with substantially less error compared to that of the SMDM by Dobson *et al.*, provided that the soils to predict the CDC are other than those used to develop each model. The MBSDM retained the good predictive accuracy of the GRMDM, complementing its advantage over the SMDM in terms of less prediction error, with the convenience of its application, which is as simple as that of the SMDM. The MBSDM proposed will be further tested over the dielectric data available to determine more accurately the domain of its applicability in terms of the variety of natural soil types.

Acknowledgment

The authors are grateful to the reviewer who suggested to test the MBSDM with regard to the soils whose dielectric data have not been used for its training.

REFERENCES

[1] M. C. Dobson, F. T. Ulaby, M. T. Hallikainen, and M. A. El-Rayes, "Microwave dielectric behavior of wet soil—Part II: Dielectric mixing models," *IEEE Trans. Geosci. Remote Sens.*, vol. GRS-23, no. 1, pp. 35–46, Jan. 1985.

[2] N. A. Peplinski, F. T. Ulaby, and M. C. Dobson, "Dielectric properties of soils in the 0.3–1.3 GHz range," *IEEE Trans. Geosci. Remote Sens.*, vol. 33, no. 3, pp. 803–807, Mar. 1995.

[3] N. A. Peplinski, F. T. Ulaby, and M. C. Dobson, "Correction to 'Dielectric properties of soils in the 0.3–1.3-GHz range'," *IEEE Trans. Geosci. Remote Sens.*, vol. 33, no. 6, p. 1340, Jun. 1995.

[4] V. L. Mironov, M. C. Dobson, V. H. Kaupp, S. A. Komarov, and V. N. Kleshchenko, "Generalized refractive mixing dielectric model for moist soils," in *Proc. IGARSS*, Toronto, ON, Canada, 2002, vol. VI, pp. 3556–3558.

[5] V. L. Mironov, M. C. Dobson, V. H. Kaupp, S. A. Komarov, and V. N. Kleshchenko, "Generalized refractive mixing dielectric model for moist soils," *IEEE Trans. Geosci. Remote Sens.*, vol. 42, no. 4, pp. 773–785, Apr. 2004.

[6] J. R. Birchak, C. G. Gardner, J. E. Hipp, and J. M. Victor, "High dielectric constant microwave probes for sensing soil moisture," in *Proc. IEEE*, Jan. 1974, vol. 62, pp. 92–98.

[7] V. L. Mironov, S. A. Komarov, N. V. Rychkova, and V. N. Kleshchenko, "Study of the dielectric properties of wet grounds at microwave frequencies," *Earth Obs. Remote Sens.*, vol. 12, no. 4, pp. 495–504, 1995.

[8] J. R. Wang and T. J. Schmugge, "An empirical model for the complex dielectric permittivity of soils as a function of water content," *IEEE Trans. Geosci. Remote Sens.*, vol. GRS-18, no. 4, pp. 288–295, Apr. 1980.

[9] V. L. Mironov, "Spectral dielectric properties of moist soils in the microwave band," in *Proc. IGARSS*, Anchorage, AK, 2004, vol. V, pp. 3474–3477.

[10] V. L. Mironov and P. P. Bobrov, "Soil dielectric spectroscopic parameters dependence on humus content," in *Proc. IGARSS*, Toulouse, France, 2003, vol. II, pp. 1106–1108.

[11] V. L. Mironov, V. H. Kaupp, S. A. Komarov, and V. N. Kleshchenko, "Frozen soil dielectric model using unfrozen water spectroscopic parameters," in *Proc. IGARSS*, Toulouse, France, 2003, vol. VII, pp. 4172–4174.

[12] V. L. Mironov, P. P. Bobrov, and V. N. Mandrygina, "Bound water spectroscopy for the soils with varying mineralogy," in *Proc. IGARSS*, Anchorage, AK, 2004, vol. V, pp. 3478–3480.

[13] V. L. Mironov, S. A. Komarov, and V. N. Kleshchenko, "Microwave dielectric spectroscopy for bound water in saline soil," in *Proc. IGARSS*, Seoul, Korea, 2005, vol. V, pp. 3196–3199.

[14] V. L. Mironov, P. P. Bobrov, A. P. Bobrov, V. N. Mandrygina, and V. D. Stasuk, "Microwave dielectric spectroscopy of moist soils for a forest–tundra region," in *Proc. IGARSS*, Seoul, Korea, 2005, vol. VII, pp. 4485–4488.

[15] V. L. Mironov, P. P. Bobrov, L. G. Kosolapova, V. N. Mandrygina, and S. V. Fomin, "Data processing technique for deriving soil water spectroscopic parameters in microwave," in *Proc. IGARSS*, Denver, CO, 2006, vol. VI, pp. 2957–2961.

[16] J. Sabburg, J. A. R. Ball, and N. H. Hancock, "Dielectric behavior of moist swelling clay soils at microwave frequencies," *IEEE Trans. Geosci. Remote Sens.*, vol. 35, no. 1, pp. 784–787, Jan. 1997.

[17] J. O. Curtis, C. A. Weiss, Jr., and J. B. Everett, "Effect of soil composition on dielectric properties," U.S. Army Corps Eng. Waterways Exp. Station, Vicksburg, MS, Dec. 1995.

[18] M. T. Hallikainen, F. T. Ulaby, M. C. Dobson, M. A. El-Rayes, and L.-K. Wu, "Microwave dielectric behavior of wet soil—Part I: Empirical model and experimental observations," *IEEE Trans. Geosci. Remote Sens.*, vol. GRS-23, no. 1, pp. 25–34, Jan. 1985.

[19] F. T. Ulaby, R. K. Moor, and A. K. Fung, *Microwave Remote Sensing: Active and Passive*, vol. III. Dedham, MA: Artech House, 1986. Appendix E-2.

Valery L. Mironov (M'98) received the M.S. and Ph.D. degrees in radio physics from Tomsk State University, Tomsk, Russia, in 1961 and 1968, respectively, and the Full Professor degree in radio physics from the Russian Academy of Sciences, Moscow, Russia, in 1984.

Currently, he is a Laboratory Head with the Kirensky Institute of Physics, Siberian Branch, Russian Academy of Sciences (SB RAS), Krasnoyarsk, Russia. From 1961 to 2004, he was a Senior Scientific Worker, Laboratory Head, Full Professor, and Chair Head with Tomsk State University; Altai State University, Barnaul, Russia; Institute of Atmospheric Optics, SB RAS; and Krasnoyarsk Science Center, SB RAS. He was also a Deputy Director of Research with the Institute of Atmospheric Optics from 1982 to 1986 and the President of Altai State University from 1986 to 1997. As a Visiting Scientist, he was with the University of British Columbia, Vancouver, BC, Canada, and the Geophysical Institute, University of Alaska, Fairbanks, in 1997/1998 and 2001, respectively, receiving a position of Affiliate Professor of Geophysics. He is the author or coauthor of over 260 scientific publications and 6 books, including *Generalized Refractive Mixing Dielectric Model for Moist Soils* (IEEE Trans. Geosci. Remote Sens., 2004), *Microwave Remote Sensing of Soils* (in Russian) (SB RAS, 2000), and *Lidar in a Turbulent Atmosphere* (Artech House, 1987). His current research interests include electromagnetic-wave propagation and scattering linked to radar and radio thermal microwave remote sensing of land and boreholes, including the studies of dielectric properties of moist soils and litter, as well as fluidized rocks pertaining to oil wells. Previously, the area of his research included the problems of laser beam propagation through the atmosphere and laser remote sensing of a turbulent atmosphere, with high-energy laser beams being concerned.

Prof. Mironov is a member of the Russian Academy of Sciences and the International Academy of Higher Education. He was the recipient of the USSR State Award in Science and Engineering, the SB RAS Award in Applied Research, the title of Honorable Professor at Altai State University, and the Altai State Award in Science and Engineering in 1985, 1987, 1997, and 1999, respectively. He is a Reviewer for the editorial board of the IEEE TRANSACTIONS ON GEOSCIENCE AND REMOTE SENSING.

Lyudmila G. Kosolapova received the M.S. degree in mathematics from Krasnoyarsk State University, Krasnoyarsk, Russia, in 1971 and the Ph.D. degree in biophysics from the Institute of Biophysics, Siberian Branch, Russian Academy of Sciences (SB RAS), Krasnoyarsk, in 1979.

She is currently a Senior Researcher with the Radiophysics of Remote Sensing Laboratory, L. V. Kirensky Institute of Physics, SB RAS. Her research interests include simulation of the microwave dielectric properties of soils, data processing, and dielectric models testing. She is the author or coauthor of over 60 scientific publications.

Sergej V. Fomin was born in Divnogorsk, Russia, in 1979. He received the M.S. degree in radio engineering from Krasnoyarsk State Technical University, Krasnoyarsk, Russia, in 2002.

He is currently an Engineer with the L. V. Kirensky Institute of Physics, Siberian Branch, Russian Academy of Sciences (SB RAS), Krasnoyarsk. His research interests include development and testing of spectral dielectric models for moist soils with alternating mineral contents and temperatures. He is the author or coauthor of five scientific publications.